Nuclear Physics **A514** (1990) 327-338
North-Holland

PERCOLATION VERSUS MICROCANONICAL FRAGMENTATION – COMPARISON OF FRAGMENT SIZE DISTRIBUTIONS:

Where is the liquid–gas transition in nuclei?

H.R. JAQAMAN[1,2,*], Gabor PAPP[1,3] and D.H.E. GROSS[1,4]

[1] *Hahn-Meitner-Institut, Bereich Kern- und Strahlenphysik, D-1000 Berlin, 39 Fed. Rep. Germany*
[2] *Physics Department, Birzeit University, Birzeit, West Bank*
[3] *Dept. of Theoretical Physics, Eötvös Roland Univ., Budapest, Hungary*
[4] *Fachbereich Physik der Freien Universität, Berlin, Fed. Rep. Germany*

Received 12 January 1990
(Revised 2 March 1990)

Abstract: The distributions of fragments produced by microcanonical multifragmentation of hot nuclei are compared with the cluster distributions predicted by a bond percolation model on a finite lattice. The conditional moments of these distributions are used together with the correlations between the largest three fragments in each event. Whereas percolation and statistical nuclear fragmentation agree in many details as in the usual plots of the averaged moments of the fragment distributions which yield the critical exponents, they turn out to be essentially different when less averaged quantities or correlations are considered. The differences between the predictions of the two models are mainly due to the particularities of the nuclear problem, especially the effect of the long-range Coulomb force which favours the break-up of the highly excited nucleus into two large fragments (pseudo-fission) and, to a somewhat lesser extent, enhances the possibility for the cracking of the nucleus into more than two large fragments. The fission events are, however, clearly separated from a second branch of critical correlations which shows up clearly in both nuclear fragmentation and percolation. We think that this critical correlation branch is due to the liquid-gas phase transition in finite nuclei.

1. Introduction

The break-up of very hot nuclei is presently one of the most interesting areas of research in nuclear physics. These highly excited pieces of nuclear matter can be produced in medium and high energy heavy-ion collisions and in high-energy proton-induced reactions. Such events are characterized, especially in the more violent collisions, by the production of a large number of fragments which are thought to result from the disassembly of the hot nuclei produced in the collision. Several approaches have been utilized to study the disassembly of such hot nuclei:

(i) The statistical decay of equilibrated very hot nuclei which starts from the statistical mechanical assumption that the phase space available to the hot nucleus is populated uniformly. There have been several calculations along this line [1-3]) in

* Alexander von Humboldt fellow.

0375-9474/90/$03.50

a canonical as well as a microcanonical ensemble. However, by assuming equilibration, these models cannot provide any information about the dynamics of the fragment formation process. The occurrence of a phase transition in these statistical models has been observed and discussed by Gross and coworkers (see also ref. [4])) and Bondorf and his coworkers (see also ref. [5])).

(ii) Various models of liquid-gas transitions that see the break-up of the hot nucleus as a reflection of a liquid-gas transition near the critical temperature T_c of nuclear matter [6,7]). The occurrence of the liquid-gas transition in nuclear matter and the associated phase instabilities that may be reflected in nuclear fragmentation have been discussed by many authors [8-14]). Theoretical studies indicate that infinite nuclear matter behaves like a Van der Waals gas with a critical temperature of 15-20 MeV [refs. [8,12])]. For temperatures $T < T_c$ an infinite cluster (liquid) coexists with its vapor whereas above T_c only small clusters and single particles can exist. However, finite size and Coulomb effects may modify this transition drastically [15-17]).

(iii) Percolation models have also been used to describe nuclear fragmentation [18-20]). The picture of the nucleus in this approach is that of a single connected cluster of nucleons. During the collision bonds between these nucleons may be broken and the nucleons that remain bonded together in a finite nuclear volume form clusters that correspond to the observed fragmentation products. The problem is then analogous to that of bond percolation on a finite lattice where all the lattice sites are occupied and the probability of having a bond between two neighboring sites is denoted as p. If p is greater than a critical value p_c it is found that there is one big cluster that percolates through the whole lattice, while for $p < p_c$ only small clusters can exist. This approach is interesting for several reasons. For one, percolation is an especially simple model for phase transitions, depending only on local geometry, so that deviations of the nuclear system from the percolation predictions can be seen to reflect the importance of the long-range Coulomb force. Moreover, percolation provides a useful method to study the fragment distributions namely, to calculate the conditional moments of the fragment distribution for each event. These moments have been used to investigate the percolation phase transition and to elucidate the critical exponents that characterize its critical point. The calculation of these moments allows for a comparison between the percolation transition and any phase transition that may occur in hot nuclei. This is quite useful since nuclei as a result of the Coulomb force are always finite so that there exists no thermodynamic limit for the nuclear system and the nature of a phase transition in such a system cannot be directly explored in contrast to percolation where the transition towards the infinite system can be easily performed. Campi [20]) has suggested an interesting approach in this regard namely, to compare nuclear data with results of percolation on finite lattices of a similar size. This method is expected to deal, at least partially, with the problem of the finite size of nuclear systems.

Here it must be noted that the percolation model used in the present paper has no isospin degrees of freedom since we are not interested in the isotopic distribution of the fragments and since including such degrees of freedom may be an unwarranted

complication of the percolation model for the purposes of the present work. It must be mentioned though that the inclusion of such degrees of freedom in the percolation model can and has been done [21]).

2. Calculations and results

The normalized kth moment of the fragment size distribution of a single event is defined as [20])

$$S_k = \sum m(s)s^k / \sum m(s)s \tag{1}$$

where $m(s)$ is the multiplicity of the fragments of size s and the summation runs over all fragments except the heaviest one s_{m1} which is considered to be the equivalent of the infinite percolation cluster that exists for infinite systems above the percolation threshold. These moments are to be calculated for each event separately. Campi [20,22]) has compared plots of averaged moment distributions for percolation on cubic 6^3 and 5^3 lattices with similar plots for the charge moment distributions of fragments of 367 experimental events obtained from the break-up of high-energy gold nuclei ($Z = 79$) impinging on emulsion [23]). This data is inclusive data since no attention is given to the amount of energy deposited in the gold nucleus. He tried to elucidate from these moment distributions the critical exponents of the phase transitions that occur in these systems and came to the conclusion that the nuclei break up like finite systems that show a phase transition in the thermodynamic limit but was not able to determine the nature of the phase transition for the nuclear case although the critical exponents obtained were close to those that occur in liquid-gas and percolation phase transitions. Better data with much more statistics is however needed for a definite classification of the phase transition.

We have calculated the distributions of the averaged moments also within the statistical model of microcanonical nuclear fragmentation. There is a remarkable similarity in the various correlations for the averaged moments between percolation and nuclear fragmentation as has already been observed in earlier calculations [20,24]). Certainly this indicates a high degree of similarity in the critical behaviour of both systems. However, if one is interested in the effects of the different natures of the forces in the two models (local order between nearest neighbours as opposed to long-range Coulomb forces) then the details of the distributions of these moments provide the answer as they contain a wealth of information especially if these moments are not averaged in any way. In the absence of experimental data with sufficient statistics the present work is mainly devoted to comparing the event moment distributions for percolation and for microcanonical nuclear fragmentation [2]).

Fig. 1 is a log-log plot of the largest fragment charge Z_{m1} in each event versus the corresponding second moment S_2 of the event for the fragment charge distributions of gold nuclei obtained in a microcanonical Metropolis sampling calculation that includes sequential proton evaporation [25]) and has an excitation energy distribution that simulates experimental proton-nucleus data [23]). Fig. 2 is a similar plot of

the largest fragment s_{m1} versus S_2 for percolation on a cubic 4^3 lattice. The sizes of the two systems are slightly different (64 percolation sites as compared to $Z = 79$ for gold nuclei) and this accounts for some of the differences between the two plots like the largest value for Z_{m1} (or s_{m1}). Both plots have similar features namely, they consist of two branches: the upper branch with high values for Z_{m1} (or s_{m1}) corresponds, in the nuclear case, to $T < T_c$ and, in the percolation case, to $p > p_c$; while the lower branch corresponds to $T > T_c$ and $p < p_c$, respectively. The different colors used in these and the following figures reflect the division of the various events into 4 different types depending on the number n of fragments in the event with charge (or size) greater than or equal to a certain threshold value, Zth (or sth) here taken to be 5. Each event is classified a pseudo-evaporation, a pseudo-fission, a cracking or a vaporization event if $n = 1$, $n = 2$, $n > 2$ or $n = 0$, respectively [26]).

There is a difference, however, in the details of the structure of the moment distributions predicted by percolation and microcanonical nuclear multifragmentation as can be seen by examining figs. 1 and 2. In particular in the nuclear case there is an additional concentration of events that are marked by large values for both Z_{m1} and S_2. These are pseudo-fission events in which two large fragments are produced as can be seen from the colored plots and they reflect a specific feature of the nuclear case namely, the existence of the long-range Coulomb force whereas percolation is governed by local geometrical properties.

It must be stressed that these fission events are not cold-fission events since the energy deposited in the nucleus in such events is at least 200 MeV and can be as high as 800 MeV. This is also verified by considering the charged-fragment multiplicity which is found for the events with lowest energy to be 6.1 on the average (in addition to 4.6 neutrons) and increases to 21.2 charged fragments (and 14.1 neutrons) for an excitation energy of 800 MeV. If these fission events are excluded from fig. 1 then the upper and lower branches in nuclear fragmentation are very similar to the corresponding branches in percolation indicating that these branches represent the respective phase transitions (the liquid–gas transition in the nuclear case versus the percolation phase transition). It is from the slopes of these branches that the critical exponents of the phase transitions must be evaluated. Averaging over events with the same value of Z_{m1} as has been done in refs. [20,24]) would mix the fission events with the upper-branch events.

Furthermore the details of the upper and lower branches seem to be different in figs. 1 and 2 with the peaks occuring at different places and the percolation lower branch extending all the way down to the origin. This difference is, however, not very serious and is mainly due to the uniform probability distribution used in the percolation calculations. To test how much the results depend on the probability distribution, we have carried out several percolation calculations with various differently-weighted probability distributions and found that, whereas the details of the two branches depend on the distribution being used and can be made to look more similar to the corresponding branches in the nuclear case, their slopes, which yield the critical exponents, are always independent of the distribution.

In fig. 3 the logarithm of the product of the two largest charges is plotted versus the logarithm of the corresponding second moment S_2', which is obtained by excluding the largest two charges from the summations in eq. (1). Fig. 4 is a similar plot for the heaviest two fragments in percolation. An interesting feature of such a plot is that the fission events are cleanly separated from the other types of events. It is clear that the fission peak that appears prominently in the nuclear case is completely absent in the percolation case. The separation of the events into four types depends on the threshold charge (or size) used and the appearance of well-separated peaks for fission and evaporation in fig. 3 indicates that this separation is more or less independent of the threshold size. The situation is different however for the lower ridge (which is the equivalent of the lower branch in figs. 1 and 2) where a gradual transition from one type to another indicates a certain sensitivity to the threshold size used. For a threshold size of 12 the lower ridge consists almost entirely of vaporization events.

The differences between the predictions of percolation and nuclear multifragmentation also appear in a triangular plot of the correlations between the largest three fragments in each event. These are shown in figs. 5 and 6 where only events with at least one fragment with charge (size) greater than or equal to the threshold value Z_{th} (or s_{th}) are included, that is vaporization events are excluded. In the upper corner of the triangle there is a concentration of evaporation events in which the largest fragment is much larger than the two next largest fragments while in the lower righthand corner there is a clustering of cracking events in which the three fragments are all of comparable size and all greater than Z_{th} (or s_{th}) together with pseudo-fission and pseudo-evaporation events in which the three largest fragments are close to the threshold value. In the right-angled corner one finds the fission events in which the largest two fragments are of comparable size and much larger than the third one Z_{m3} (or s_{m3}). The hypotenuse of the triangle corresponds to events in which the second and third fragments are equal.

For the evaporation events both models seem to give almost similar distributions although a careful examination of the details of the evaporation peak in the upper corner shows some noticeable differences. Moreover, percolation appears to produce much less cracking events than the nuclear multifragmentation model, as can be seen by examining the lower right-hand corner, and the fission peak is completely absent in percolation.

It is also of interest to compare these triangular plots with a similar plot, fig. 7, for the available experimental data [23,27]). Keeping in mind the difference in statistics, only 367 experimental events as compared with several million events for the theoretically-generated plots, it is nevertheless obvious that the experimental points have a much better correlation with the nuclear multifragmentation model than with percolation. In particular percolation predicts very few events in a wide area around the right-angled corner of the triangle which is contradicted by both the data and the results of the nuclear multifragmentation model as can be seen by comparing figs. 5 and 7, where a close similarity exists between the two plots in this particular

Fig. 1. The logarithm of the largest fragment charge Z_{m1} produced per event as a function of the logarithm of the corresponding second moment S_2 for the microcanonical multifragmentation of hot ^{197}Au nuclei. The plot represents 10^7 such events and the size of the character plotted at each point is proportional to the number of events belonging to that point. To enhance the details of the plot, the intensity maximum which occurs at the upper most left point of the plot has been suppressed by a factor of 32. The different colours reflect the division of the events into four types as explained in the text, with black, red, green, and blue representing pseudo-evaporation, pseudo-fission, cracking and vaporization events, respectively.

Fig. 2. The same as fig. 1 but for 2 million events of bond percolation on a cubic 4^3 lattice with uniformly distributed values of the bond probability $0 < p < 1$. Here s_{m1} is the largest percolation cluster per event. Because percolation for high values of p tends to produce single clusters that span the whole lattice, only about 1.4 million events are actually included since at least two clusters must be produced in an event in order to generate a point in this plot. This situation does not arise in the nuclear case (fig. 1). To enhance the details of the plot the intensity maximum which occurs at the uppermost left point of the plot has been suppressed by a factor of 64. Otherwise the intensities and colours have the same meaning as in fig. 1.

Fig. 3. The logarithm of the product of the largest two fragment charges $Z_{m1}Z_{m2}$ produced per event as a function of the logarithm of the corresponding second moment S_2' of the event for the microcanonical multifragmentation of hot ^{197}Au nuclei. The plot represents the same events as in fig. 1. The intensity maximum has been suppressed by a factor of 16. Otherwise the intensities and colours have the same meaning as in fig. 1.

Fig. 4. The logarithm of the product of the largest two fragments $s_{m1}s_{m2}$ produced per event as a function of the logarithm of the corresponding second moment S_2' of the event for percolation events on a cubic 4^3 lattice with uniformly distributed values $0 < p < 1$. The events used to generate this plot are the same as those that are used in fig. 2 but, since at least three fragments must be produced in each event used for this plot, only about 1.2 million events are actually plotted. The intensity maximum has been suppressed by a factor of 32. Otherwise the intensities and colours have the same meaning as in fig. 1.

Fig. 5. Triangular plot of the correlations of the largest three fragment charges in each event in the microcanonical multifragmentation of a hot ^{197}Au nucleus. The difference between the largest two charges is plotted versus the third charge. Each charge is normalized by dividing it by the sum of the three charges in the event $Z_T = Z_{m1} + Z_{m2} + Z_{m3}$. The plot represents the same events as in figs. 1 and 2 but the vaporization events have been excluded. The intensity maximum has been suppressed by a factor of 16. Otherwise the intensities and colours have the same meaning as in fig. 1.

Fig. 6. Triangular plot of the correlations of the largest three fragments in each event for percolation on a cubic 4^3 lattice with uniformly distributed values $0 < p < 1$. The events used to generate this plot are the same as those that are used in Figures 2 and 4 but the vaporization events have been excluded. The difference between the largest two fragments is plotted versus the third fragment. Each fragment is normalized by dividing it by the sum of the three fragments in the event $s_T = s_{m1} + s_{m2} + s_{m3}$. The intensity maximum has been suppressed by a factor of 16. Otherwise the intensities and colours have the same meaning as in fig. 1.

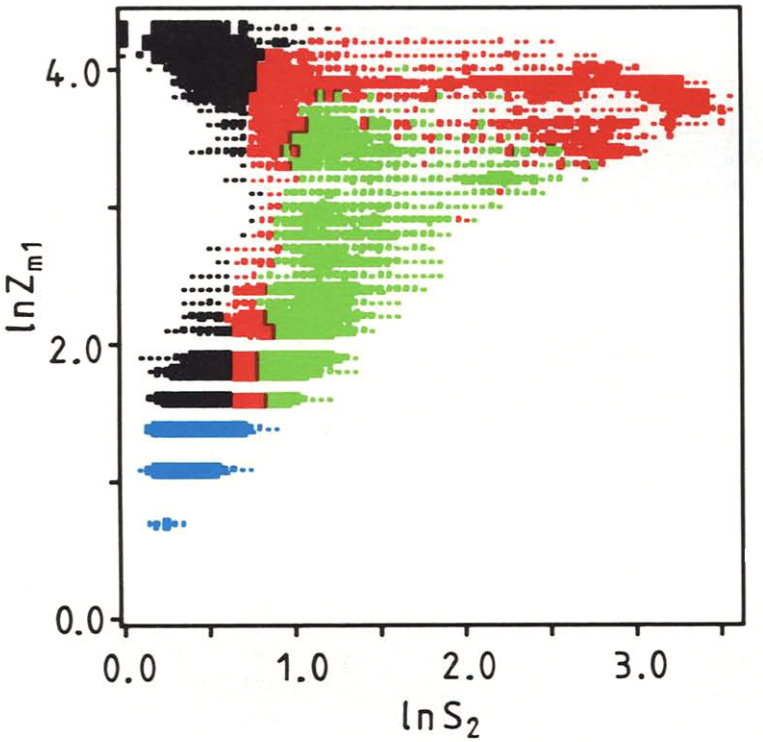

Fig. 1.

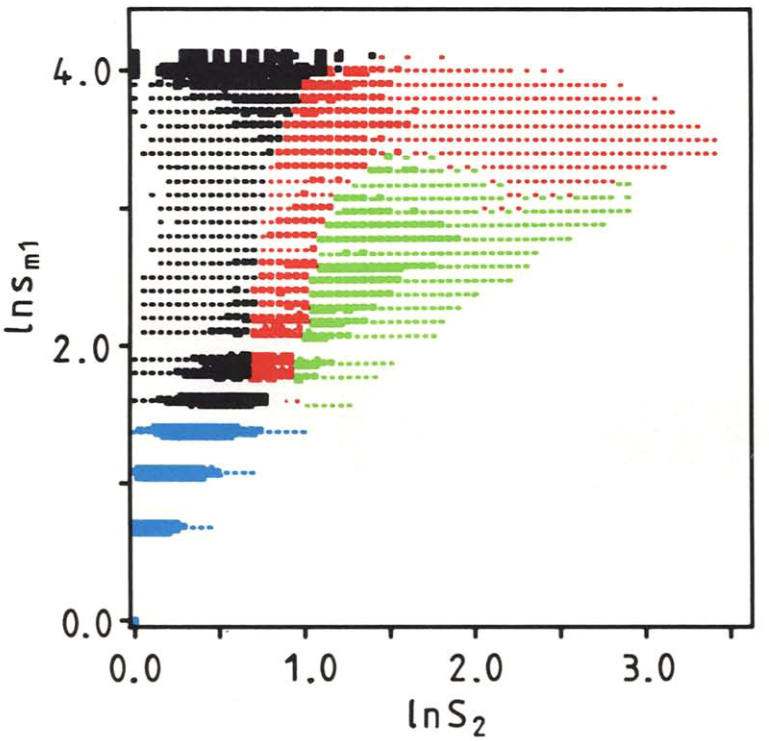

Fig. 2.

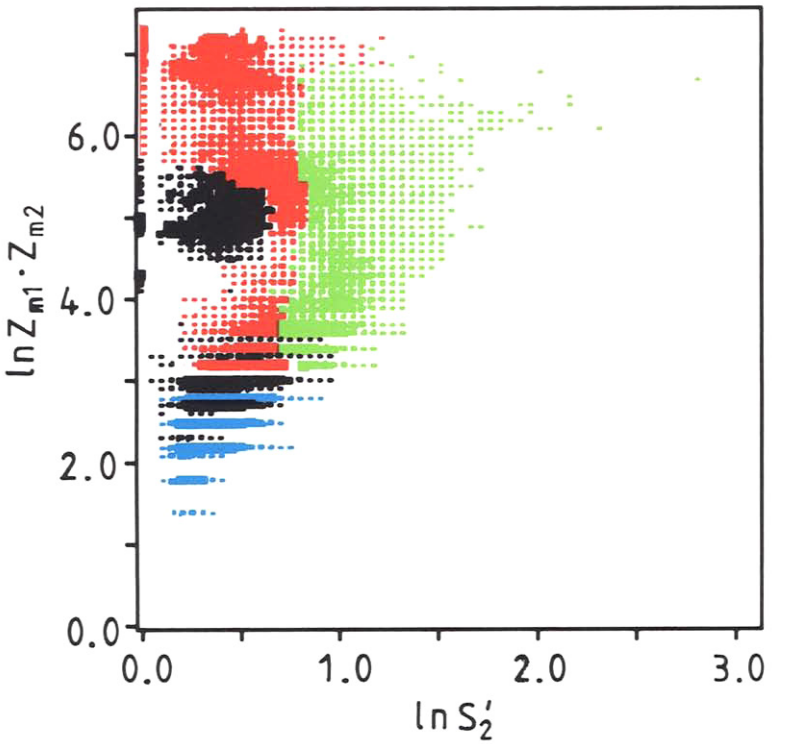
6.0
4.0
2.0
0.0
0.0
1.0
2.0
3.0
ln Zm1·Zm2
ln S2'

Fig. 3.

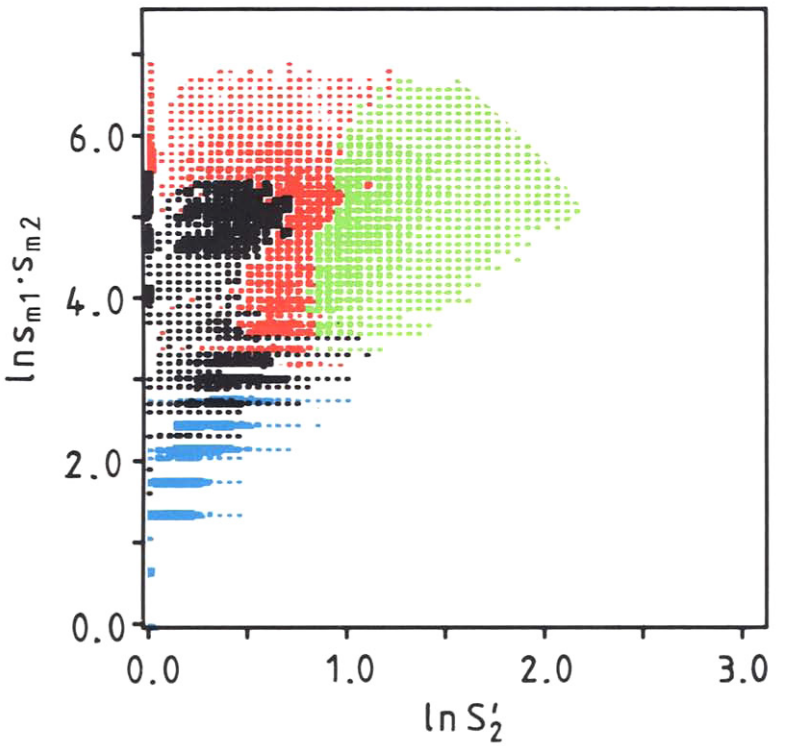
6.0
4.0
2.0
0.0
0.0
1.0
2.0
3.0
ln sm1·sm2
ln S2'

Fig. 4.

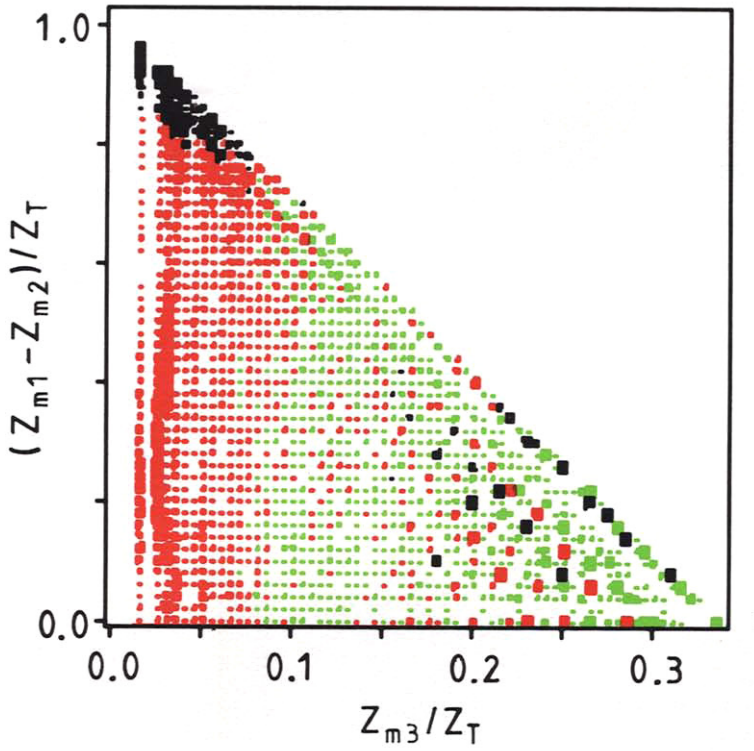
1.0
0.0
0.0
0.1
0.2
0.3
$(Z_{m1}-Z_{m2})/Z_T$
Z_{m3}/Z_T

Fig. 5.

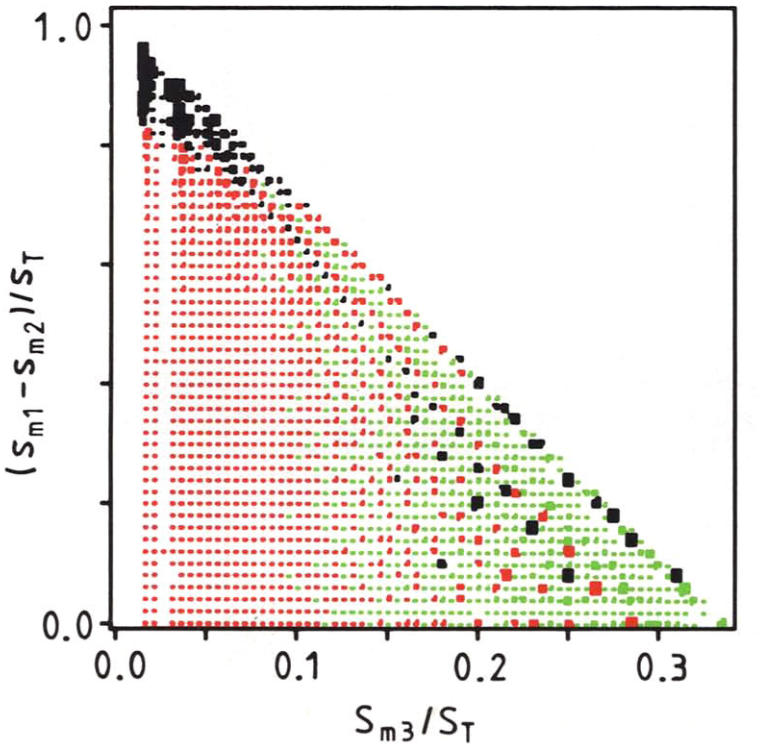
1.0
0.0
0.0
0.1
0.2
0.3
$(S_{m1}-S_{m2})/S_T$
S_{m3}/S_T

Fig. 6.

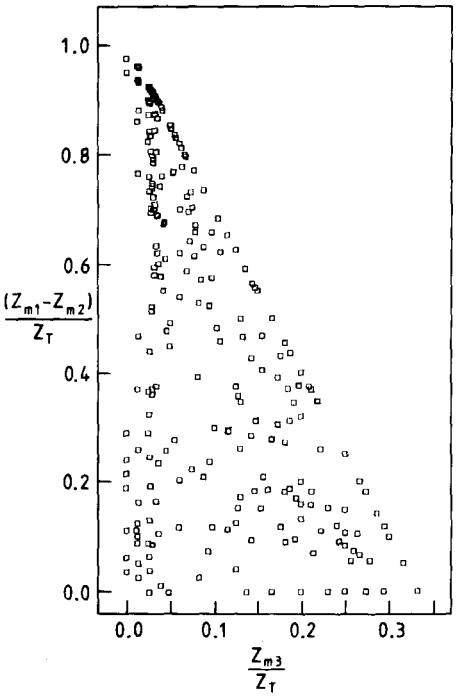

Fig. 7. Experimental data for the correlations between the three largest fragment charges from high-energy proton-induced break-up of ^{197}Au nuclei, plotted in the same way as in figs. 5 and 6.

corner. Moreover, a careful examination of the evaporation peak shows that even its details are similar in these two figures and different from those predicted by percolation, see fig. 6. In addition to the triangular plots, it is also possible to make other types of plots ($\ln Z_{m1}$ versus $\ln S_2$ and $\ln (Z_{m1}Z_{m2})$ versus $\ln S_2'$) for the experimental data. These tend to be in general agreement with the predictions of the statistical nuclear fragmentation model although the poor statistics of the experimental events prevents a more definite conclusion.

3. Conclusion

The second moment $\langle \ln S_2 \rangle$ of the charge distribution in a single event of nuclear break-up, averaged over all events with the same largest fragment charge, shows close similarity to the equivalent quantity in bond percolation on a finite lattice of similar size [20]). Only the fluctuating nonaveraged $\ln S_2$ shows important differences between statistical nuclear fragmentation and percolation. In both (see figs. 1 and 2) we find a curved mountain ridge that starts at large Z_{m1} (or s_{m1}) and $\ln S_2 = 0$ with a negative slope then bends near $\ln Z_{m1} = 3$, $\ln S_2 = 1$ and continues towards the origin with a positive slope. We suggest that in the nuclear case the

region at which this bending occurs is the critical region of the liquid-gas transition in finite nuclei. Additionally there is a second peak on a nearly horizontal mountain ridge in the nuclear case which is entirely due to pseudo-fission events that are totally absent in percolation. This additional ridge is the fingerprint of the long-range Coulomb force in the nuclear case. By carefully comparing nuclear break-up with percolation on finite lattices, as has been suggested in ref. [20]), it has therefore been possible to identify the liquid-gas transition in finite nuclei.

The comparison with the available experimental data shows remarkable similarity between it and the predictions of microcanonical nuclear fragmentation for the three-body correlations involving the largest three charges especially in the enhancement of the pseudo-fission and, to a somewhat lesser extent, the cracking events. This again emphasizes the role of the Coulomb force which tends to produce larger fragments in order to reduce the Coulomb repulsion energy between the fragmentation products whereas percolation tends to produce smaller fragments for the physically interesting ranges of p. The availability of experimental data with a much higher number of events would be most welcome in order to make these conclusions about the nature of the break-up of hot nuclei more definite.

Many interesting discussions with X. Campi are gratefully acknowledged as well as his continuous interest in this work and especially his help in evaluating the experimental material. One of the authors (H.R.J.) would like to thank the Alexander von Humboldt Foundation for financial support and the Hahn-Meitner-Institut for its hospitality. G.P. thanks the "Stabsabteilung Internationale Beziehungen, Karlsruhe, Germany" for support through the bilateral cooperation BRD/Hungary.

References

1) J. Randrup and S.E. Koonin, Nucl. Phys. **A356** (1981) 223;
S.E. Koonin and J. Randrup, Nucl. Phys. **A474** (1987) 173;
G. Fai and J. Randrup, Nucl. Phys. **A487** (1988) 397
2) D.H.E. Gross and Sa Ban-hao, Nucl. Phys. **A437** (1985) 643;
X.-Z. Zhang, D.H.E. Gross, S.-Y. Xu and X.-M. Zheng, Nucl. Phys. **A461** (1987) 641; 668
3) J.P. Bondorf, R. Donangelo, I.N. Mishustin and H. Schulz, Nucl. Phys. **A444** (1985) 460;
H.W. Barz, J.P. Bondorf, R. Donangelo, I.N. Mishustin and H. Schulz, Nucl. Phys. **A448** (1986) 753
4) D.H.E. Gross, invited talk, 1984 INS-Riken Int. Symp. on heavy-ion physics, J. Phys. Soc. Jpn. Suppl. **54** (1985) 392
5) J.P. Bondorf, R. Donangelo, H. Schulz and K. Sneppen, Phys. Lett. **B162** (1985) 30
6) A.D. Panagiotou, M.W. Curtain, H. Toki, D.K. Scott and P.J. Siemens, Phys. Rev. Lett. **52** (1984) 496
7) A.L. Goodman, J.I. Kapusta and A.Z. Mekjian, Phys. Rev. **C30** (1984) 851
8) G. Sauer, H. Chandra and U. Mosel, Nucl. Phys. **A264** (1976) 221
9) D.Q. Lamb, J.M. Lattimer, C.J. Pethick and D.G. Ravenhall, Phys. Rev. Lett. **41** ((1978) 1623
10) P. Danielewicz, Nucl. Phys. **A314** (1979) 465
11) H. Schulz, L. Münchow, G. Röpke and M. Schmidt, Phys. Lett. **B119** (1982) 12
12) H.R. Jaqaman, A.Z. Mekjian and L. Zamick, Phys. Rev. **C27** (1983) 2782
13) M.W. Curtain, H. Toki and D.K. Scott, Phys. Lett. **B123** (1983) 289
14) G. Bertsch and Philip J. Siemens, Phys. Lett. **B126** (1983) 9

15) D.H.E. Gross, L. Satpathy, Meng Ta-chung and M. Satpathy, Z. Phys. **A309** (1982) 41
16) H.R. Jaqaman, A.Z. Mekjian and L. Zamick, Phys. Rev. **C29** (1984) 2067;
H.R. Jaqaman, Phys. Rev. **C39** (1989) 169; **C40** (1989) 1677
17) S. Levit and P. Bonche, Nucl. Phys. **A437** (1985) 426
18) W. Bauer, D.R. Dean, U. Mosel and U. Post, Phys. Lett. **B150** (1985) 53; Nucl. Phys. **A452** (1986) 699
19) T.S. Biro, J. Knoll and J. Richert, Nucl. Phys. **A459** (1986) 692
20) X. Campi, J. of Phys. **A19** (1986) L917
21) O. Knospe, R. Schmidt and H. Schulz, Phys. Lett. **B182** (1986) 293
22) X. Campi, Phys. Lett. **B208** (1988) 351; J. de Phys. **50** (1989) 183
23) C.J. Waddington and P.S. Friar, Phys. Rev. **C31** (1985) 888
24) H.W. Barz, J.P. Bondorf, R. Donangelo and H. Schulz, Phys. Lett. **B169** (1986) 318
25) D.H.E. Gross, Reports on Progress in Physics (to be published)
26) D.H.E. Gross and X.-Z. Zhang, Phys. Lett. **B161** (1985) 43;
D.H.E. Gross, X.-Z. Zhang and S.-Y. Xu, Phys. Rev. Lett. **56** (1986) 1544
27) X. Campi, private communication